1 Effects of high count rates in a $\Delta E - E$ telescope

This document reports on the effects of high elastics count rate on a particle identification spectrum obtained from a MEGHA Gas-Silicon (Gas-PSD) telescope.

The following is a general argument applying to two equal-magnitude bi-polar amplifier output signals generated within $\approx 30\mu s$ of each other from a single detector element, such as a gas ionisation chamber or PSD. The majority of pile-up/down events correspond to two elastically scattered particles; the following assumes that this is the case.

1.1 Pulse piling profile

The sum of the two signals will vary as a function of the separation of the two peaks with the resultant double-peaked signal entering a single ADC.

Normally the ADC gate generated by this type of event would open before the rising edge of the first pulse and the peak detect circuitry would ensure that the first pulse height (PH) is digitised. Any subsequent pulses piling on top of the first would go unrecorded by the ADC.

However, if the data acquisition (DA) is enabled by an unrelated event in a **different** detector then the ADC gate can fall on any portion of the double peaked input and consequently the ADC can digitise *either* the first *or* the second peak. These unrelated triggers are generated more frequently in high count rate situations, or if a noisy signal is causing a rapid triggering of the DA.

The deduced variation in the recorded pulse height as a function of peak separation is plotted schematically in figure 1, and is called the pulse piling profile.

With the peak separation such that the second peak occurs in region-I the ADC records the pulse height of either peak as the 'true' elastics PH. No pulse piling occurs.

In region-II the second peak is formed on any 'overshoot' of the first pulse. The ADC records either the first peak as the 'true' elastics PH (during a self generated ADC gate) or the slightly larger second peak PH (during an uncorrelated ADC gate).

In region-III and IV, the second pulse forms in the negative bi-polar lobe of the first pulse. Again the ADC records either the first 'true' elastics PH or the now reduced second peak PH.

In region-V, the second pulse forms on the falling edge of the positive bi-polar lobe of the first pulse. The ADC again records either the 'true' elastics PH or the second larger peak PH. As the peak separation tends to zero the second peak PH becomes indistinguishable from the first and the sum of the two pulses tends to twice the elastics PH.

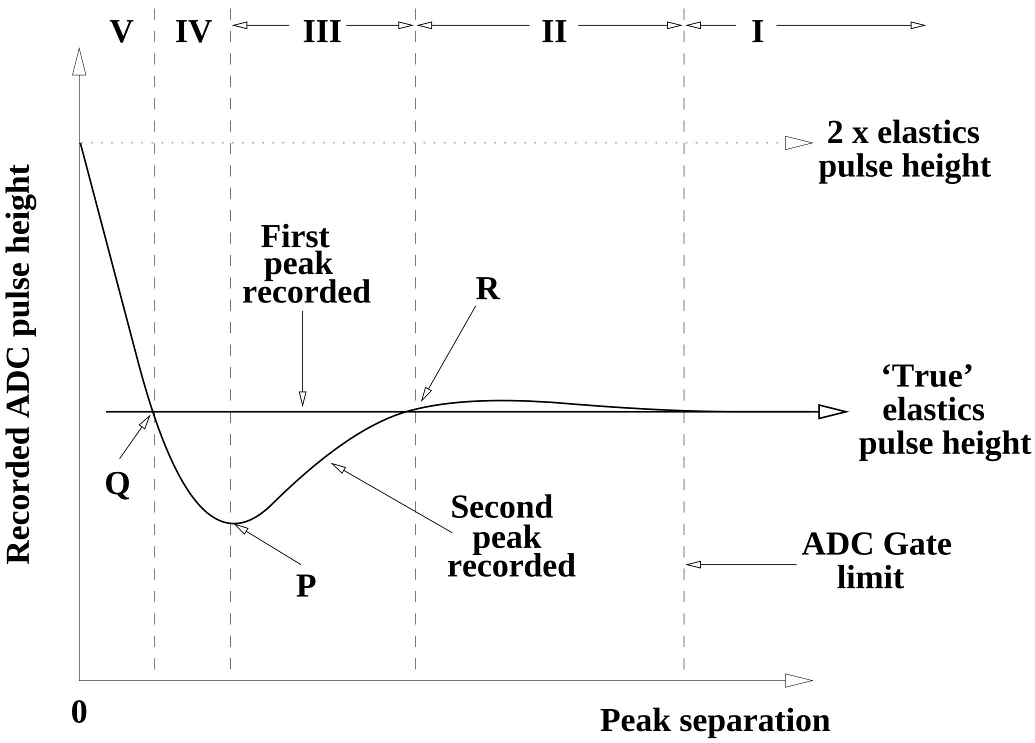

Figure 1: Double pulse piling profile.

1.2 Effects of correlated pulse piling

For two ions entering a single Gas-PSD MEGHA telescope the pulse piling profiles for both detector elements will be correlated in time. The high elastics count rate for the reaction $^{12}C+^{12}C$ at a beam energy of 60MeV in the central MEGHA module telescopes led to pulse piling in both the Gas and PSD energy signals; furthermore, noisy gas signals in two of the centre module telescopes provided an almost continuous set of random ADC gates. The rate of these unrelated ADC gates was high enough such that any internal Gas-PSD coincidence in any telescope was always accompanied by some other signal - an 'ideal' situation for pulse piling.

Figure 2(a) shows an $E\Delta E$ particle identification plot for the above reaction generated from one of the telescopes in the centre MEGHA module closest to the beam axis. With a ^{12}C beam current of $\approx$4nA the count rate in the telescope was $\approx$8kHz. Shown in figure 2(b) is a schematic highlighting areas of the $E\Delta E$ plot corresponding to either different species identification or different types of pulse piling. The origin of these areas will be explained in the following text.

The Gas signals were shaped for 1.5μs and the PSD energy signals for 5μs. Be-

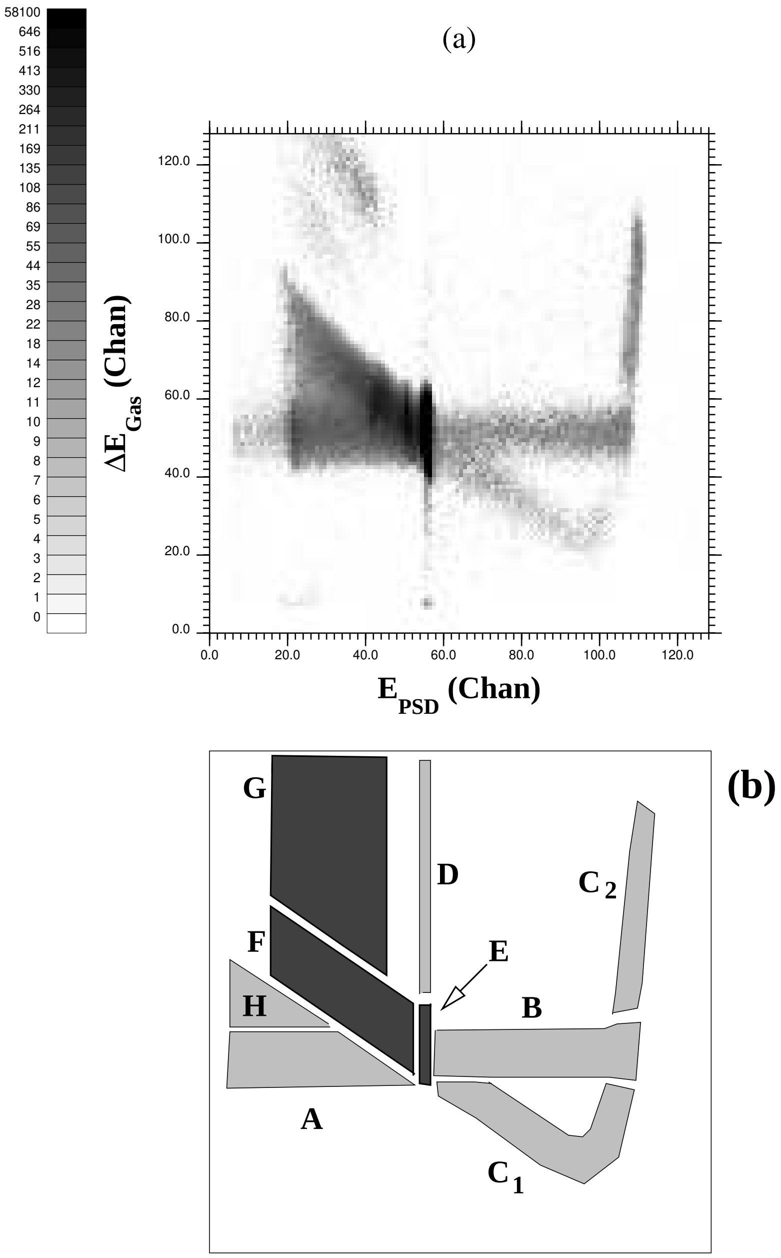

Figure 2: (a) $E\Delta E$ plot for the reaction ^{12}C+^{12}C at a beam energy of 60MeV. (b) Schematic of the $E\Delta E$ plot highlighting the different areas corresponding to different species and different types of pulse piling.

cause of the different shaping times used the pulse piling profiles for each detector element were scaled differently along the peak separation axis, such that the minimum pulse height at point "P", in figure 1, occurred at $\approx 4\mu s$ for the Gas detector and $\approx 11\mu s$ for the PSD.

For two ^{12}C ions entering the same telescope separated in time such that the piling profile is in region-I for both the gas detector and PSD, then the 'true' elastics peak is measured. This corresponds to area "E" in the schematic $E\Delta E$ plot in figure 2(b).

As the peak separation decreases such that the PSD piling profile is in region-II or III, then the corresponding Gas profile will still be in region-I. This correlation is seen in the $E\Delta E$ plot as a broad band extending down in PSD energy from the elastics peak at the constant Gas elastics energy. This is labeled as band "A" in the schematic $E\Delta E$ plot.

As the peak separation decreases further then the piling profile for the PSD enters region-IV as the corresponding Gas profile enters region-II. Any overshoot in the bipolar Gas signals will show up as a broadening of band "A" into area "H" of the schematic $E\Delta E$ plot.

As the PSD pulse piling profile enters the pile-up region-V the measured PH crosses the 'true' elastics PH at point "Q" just as the corresponding Gas piling profile enters the pile-down region-III at the point "R". The corresponding area of the schematic $E\Delta E$ plot is again the elastics area "E". As the PSD signals continue to pile-up with decreasing peak separation the corresponding ADC output for the Gas detector moves through the regions-III and IV. The correlation between the two output signals shows on the schematic $E\Delta E$ plot as region "B" where the Gas ADC records the first ^{12}C gas signal, or as region "C_1" in which the Gas ADC records the second ^{12}C pile-down signal.

For two ^{12}C ions entering the telescope almost in exact coincidence then the PSD signal tends to approximately twice the elastics PH and the Gas ADC output for region-V gives a single value tending rapidly towards twice the Gas elastics PH. This correlation appears in the $E\Delta E$ schematic as area "C_2".

Other areas of the $E\Delta E$ plot are;

- D: An elastically scattered particle entering telescope in coincidence with a low energy particle which stops in the gas volume; leads to a 'true' PSD elastics PH and a higher than elastics Gas PH,
- F: Inelastically scattered ^{12}C ions,
- G: Other species produced in the reaction.

The summed number of counts occurring in the areas "A,B,C_1,C_2 and H" account for approximately 8% of the total. This fraction is dependent on the signal shaping times, ADC gate width, telescope count rate and the presence of noisy signals. The signal piling effects seen in figure 2(a) represent the worst case yet seen.

A separate experiment was performed, in which the PSD energy and Gas signals were both shaped for $5\mu s$. The central MEGHA module was again used with a 200MeV beam of ^{35}Cl scattered off a ^{197}Au target giving a high elastics count rate. The use of similar shaping times in both elements gave a different pulse piling correlation to that described previously; the $E\Delta E$ plot for one of the telescopes is shown in figure 3. The pulse piling profiles for the two elements are almost exactly correlated in time.

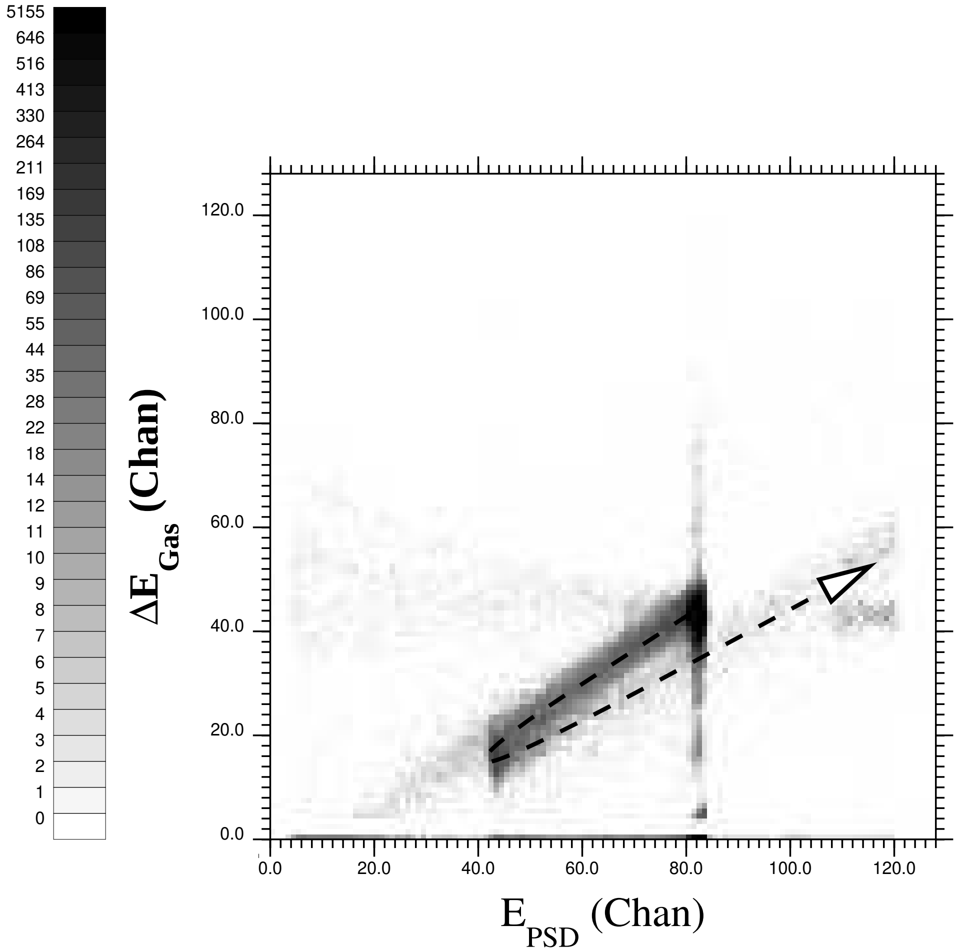

Figure 3: $E\Delta E$ plot for the reaction ^{35}Cl+^{197}Au at a beam energy of 200MeV. The arrow highlights the progression of the correlated piling signals as the peak separation decreases.

The elastics peak for non-piling events in figure 3 is clearly identifiable in channel $(E, \Delta E)$=(83,44). Now, as the peak separation decreases as before, the piling profiles for each element move through regions I,II and III in tandem leading to the band of events stretching diagonally from the elastics peak towards the bottom left hand corner of the figure.

If both piling profiles were exactly correlated as the signals started to pile-up through regions IV and V then these events would contribute to the same diagonal band, eventually extending to twice the elastics PH at channel (166,88); however, small discrepancies in the value of the amplifier components led to slightly different scaling of the peak separation axis in figure 1 for each detector element; this caused the pile-up in the Gas signal to lag behind that of the PSD energy signal. So now, as the peak separation decreases, the events move along a different diagonal band running from the bottom left to the top right of figure 3 and passing just beneath the elastics peak. This correlation terminates at channel (122,58) due to the PSD signal falling outside the ADC conversion range. The arrow in figure 3 highlights the progression of the correlated signals as the peak separation decreases.

2 Possible solutions

Reducing the number of channels which directly trigger the DA should reduce the rate of random ADC gates caused by noise. Since the Gas signals are prone to noise pick-up it would be prudent to demand a PSD energy coincidence before using them as a DA trigger.

The use of unipolar input signals to the ADC's would alter the pulse piling profile of figure 1. In this case the PH of piling elastics events would always be greater than the 'true' elastics pulse height; this would avoid contamination of other lighter ion particle identification locii by pile-down elastics events such as those in bands "A" and "H" in figure 2(a).

Another solution would be to shield the inner edges of the telescopes closest to beam by using a radial disc absorber placed around the beam axis. This has already been tried during the MEGHA commissioning and was proven successful in reducing the telescope count rate to manageable levels. However, this does reduce the detection efficiency of MEGHA which should be avoided.

Shorter shaping times would reduce the degree of piling. The Gas section can be run successfully with shaping of $1.5\mu s$, whereas the PSD's show worse energy signal ballistic deficit at lower shaping times. The newer Eurisys PSD's can be run with shorter shaping times than the Hamamatsu PSD's used in the above experiments.

For reaction data (assuming a binary coincidence requirement), a relative timing gate should be able to reject those events in which one of the break-up fragments piles on top of an **earlier**, unrelated particle in the same telescope. However, if an unrelated particle arrives **after** a break-up fragment in the same telescope this would be indistinguishable, in terms of the timing spectrum, from a true, uncontaminated coincident event.